Targeting Angiogenesis via a c-Myc/Hypoxia-Inducible Factor-1α–Dependent Pathway in Multiple Myeloma

Jing Zhang,[1,2] Martin Sattler,[1] Giovanni Tonon,[3,8] Clemens Grabher,[4] Samir Lababidi,[6] Alexander Zimmerhackl,[1,2] Marc S. Raab,[1,2] Sonia Vallet,[5] Yiming Zhou,[7] Marie-Astrid Cartron,[7] Teru Hideshima,[1] Yu-Tzu Tai,[1] Dharminder Chauhan,[1,2] Kenneth C. Anderson,[1,2] and Klaus Podar[1,2,9]

[1]Department of Medical Oncology, [2]Jerome Lipper Multiple Myeloma Center, LeBow Institute for Myeloma Therapeutics, [3]Center for Applied Cancer Science, and [4]Department of Pediatric Oncology, Dana-Farber Cancer Institute and Harvard Medical School; [5]Center for Multiple Myeloma, Massachussetts General Hospital and Harvard Medical School, Boston, Massachussetts; [6]Division of Biostatistics, Center for Devices and Radiological Health, U.S. Food and Drug Administration, Rockville, Maryland; [7]Myeloma Institute for Research and Therapy, University of Arkansas for Medical Sciences, Little Rock, Arkansas; [8]San Raffaele Scientific Institute, Milan, Italy; and [9]National Center for Tumor Diseases (NCT)/University of Heidelberg, Heidelberg, Germany

Abstract

Bone marrow angiogenesis is associated with multiple myeloma (MM) progression. Here, we report high constitutive hypoxia-inducible factor-1α (Hif-1α) expression in MM cells, which is associated with oncogenic c-Myc. A drug screen for anti-MM agents that decrease Hif-1α and c-Myc levels identified a variety of compounds, including bortezomib, lenalidomide, enzastaurin, and adaphostin. Functionally, based on transient knockdowns and overexpression, our data delineate a c-Myc/Hif-1α–dependent pathway mediating vascular endothelial growth factor production and secretion. The antiangiogenic activity of our tool compound, adaphostin, was subsequently shown in a zebrafish model and translated into a preclinical *in vitro* and *in vivo* model of MM in the bone marrow milieu. Our data, therefore, identify Hif-1α as a novel molecular target in MM and add another facet to anti-MM drug activity. [Cancer Res 2009;69(12):5082–90]

Introduction

Multiple myeloma (MM) is an incurable malignant disorder of postgerminal center B cells characterized by clonal proliferation of immunoglobulin-secreting malignant plasma cells in the bone marrow (BM). Tumor cells are extremely heterogeneous, either hypodiploid with IgH translocations or hyperdiploid with multiple trisomies and a variety of genetic mutations. In addition, the intimate reciprocal relationship between tumor cells and the cellular and noncellular microenvironment, the BM vasculature in particular, plays a pivotal role in MM pathophysiology. Vascular endothelial growth factor (VEGF), which is expressed and secreted by MM cells and increased in cocultures of MM cells with stromal cells, is the most potent angiogenic factor. Functionally, VEGF increases BM microvascular density (MVD), as well as triggers MM cell proliferation, survival, and migration in both a paracrine and autocrine manner. MVD is correlated with MM progression and poor prognosis (1).

The helix-loop-helix leucine zipper transcription factor c-Myc is a proto-oncogene associated with cell apoptosis via an ARF-Mdm2-p53 tumor suppressor pathway and loss of differentiation. Lethality in c-myc (−/−) mouse embryos is in part associated with a requirement for c-Myc for VEGF expression, as VEGF can partially rescue defects in differentiation and growth, including vasculogenesis (2). Deregulated or elevated expression of c-Myc (oncogenic c-Myc) is independent of external signals and occurs in ~30% of human cancers, including breast, colon, cervical, small cell lung cancer, osteosarcoma, glioblastoma, melanoma, and myeloid leukemias. Besides directly coordinating multiple intracellular programs that mediate metabolic activity and drive proliferation, c-Myc facilitates tumor cell growth via angiogenesis in a highly complex manner, further highlighting the intimate interrelation of tumor and microenvironment (3). Specifically, although oncogenic, c-Myc activation is accompanied by overwhelming apoptosis. It is only after suppression of c-Myc–induced apoptosis by coexpression of Bcl-xL that c-Myc triggers rapid and uniform progression into angiogenic, invasive tumors (2). Indeed, c-Myc has been postulated to be the master regulator of angiogenic factors, most prominently VEGF, and to be preeminent for the angiogenic switch required for tumor progression and metastasis (4, 5). For example, targeted skin expression of c-Myc induces VEGF protein release and, in conjunction with hypoxia, further increases VEGF protein levels and angiogenesis (6). In MM, complex karyotypic abnormalities of the c-myc locus have been reported in the majority of MM cell lines, including MM.1S, KMS-12, OPM-1, OPM-2, OCI-My5, and RPMI8226. For example, our model MM.1S cell line carries a constant region of IgH (CH) insertion and duplication of c-Myc and CH on chromosome 8 (7). Rearrangements of c-Myc are reported in nearly 40% of advanced human MM. Enforced expression of c-Myc by immunoglobulin enhancers with peak activity in plasma cells recapitulates some features of human MM in a murine model (8). Moreover, a conditional mouse model of sporadic MM strongly supports a pivotal role for c-Myc deregulation in the progression of benign MGUS to malignant MM (9). Functional mechanisms of c-Myc mediating disease progression are not fully elucidated, and a role of c-Myc in triggering MM BM angiogenesis may be a contributing factor (5, 6, 10). Consistent with this hypothesis, our own previous studies (11) show that VEGF production and secretion in MM cells is c-Myc dependent.

Hypoxia-inducible factor-1α (Hif-1α) is a prominent transcription factor regulating angiogenesis, predominantly via induction of VEGF transcription. In cancer, oxygen-independent and

Note: Supplementary data for this article are available at Cancer Research Online (http://cancerres.aacrjournals.org/).

K.C. Anderson and K. Podar contributed equally.

Requests for reprints: Klaus Podar, Dana-Farber Cancer Institute, Department of Medical Oncology, Jerome Lipper Multiple Myeloma Center, LeBow Institute for Myeloma Therapeutics, 44 Binney Street, Boston, MA 02115. Phone: 617-632-2144; Fax: 617-632-2140; E-mail: klaus_podar@dfci.harvard.edu.

doi:10.1158/0008-5472.CAN-08-4603

oxygen-dependent pathways regulate Hif-1α expression. Specifically, intratumoral hypoxia induces Hif-1α expression, which is associated with progression of cervical cancer, non–small cell lung cancer, breast cancer, and ovarian cancer. However, Hif-1α is also induced in an oxygen-independent way via growth-factor receptors or other signaling molecules to maintain oxygen homeostasis. Specifically, growth factors, signaling molecules, and loss of function mutations of molecules such as VHL, p53, and PTEN, trigger Hif-1α synthesis in stimulated cells, including cancer cells (12–14). Prior studies found that bortezomib inhibits MM adaptation by stimulating factor-inhibiting Hif-1 (15) and that inhibitor of growth family member 4 suppresses Hif-1α activity and angiogenesis under hypoxic conditions (16). Moreover, Asosingh and colleagues have suggested an important role of Hif-1α and BM hypoxia in MM progression (17).

Under physiologic conditions, Hif-1α inhibits c-Myc activity; however, when deregulated oncogenic c-Myc collaborates with Hif-1α in inducing the expression of VEGF (angiogenesis), PDK1, and hexokinase 2 (glycolysis; refs. 18, 19). The relationship between c-Myc and Hif-1α in MM and BM angiogenesis, as well as its potential as a target for novel and investigational anti-MM agents, is unknown. Our results delineate a c-Myc/Hif-1α–dependent pathway modulating MM cell production and secretion of VEGF and angiogenesis, even under normoxic conditions. Moreover, we show that the tyrophostin adaphostin (NSC680410; refs. 20–22), as well as other anti-MM agents, inhibit this c-Myc/Hif-1α–dependent pathway, VEGF secretion, and tumor angiogenesis within the MM microenvironment. Our data, therefore, identify Hif-1α as a promising novel therapeutic target in MM.

Materials and Methods

Materials. Adaphostin (NSC 680410), the adamatyl ester analogue of the tyrophostin AG957, was kindly provided by the Drug Synthesis and Chemistry Branch, Division of Cancer Treatment and Diagnosis, National Cancer Institute. Antibodies directed against c-Myc, extracellular signal-regulated kinase-2 (ERK-2), and actin were from Santa Cruz, and antibody against Hif-1α was from Cell Signaling Technology.

Cell culture. All human MM cell lines and primary patient MM cells were cultured as previously described (11). Human umbilical vein endothelial cells from a pool of five healthy donors (kindly provided by Drs. A. Cardoso and M. Tavares, Dana-Farber Cancer Institute) were maintained in EGM-2MV media (Cambrex) containing 2% fetal bovine serum. The collection and use of human tissue for this study was approved by the Internal Review Board of the Dana-Farber Cancer Institute. Informed consent was obtained in accordance with the Declaration of Helsinki.

Plasmids, small interfering RNAs, and transfections. 3× HRE luciferase plasmid was kindly provided by Drs. Q. Yan, W.G. Kaelin, and A. Kung (Dana-Farber Cancer Institute; ref. 23). For generation of the mutated 3× HRE construct, HRE sequences ACGTG were mutated to AAAAG using the Stratagene QuikChange XL site-directed mutagenesis kit (Stratagene). The integrity of the mutated 3× HRE construct was verified by sequencing. pcDNA3-cmyc plasmid 16011 (deposited by Dr. W. El-Deiry; ref. 24) was purchased from Addgene. For c-Myc– and Hif-1α–specific knockdown experiments, MM.1S cells were transiently transfected with indicated amounts of small interfering RNA (siRNA) SMARTpool of cMyc and Hif-1α or nontargeting control (mock) siRNA (Upstate Cell Signaling Solutions/Dharmacon RNA Technologies) using the Cell Line Nucleofector Kit V Solution (Amaxa Biosystems/Lonza). Nontargeting control (mock) siRNA is composed of a pool of four siRNAs, which have been characterized by genome-wide microarray analysis and found to have minimal off-target signatures.

Cell lysis and Western blotting. Cell lysis and Western blot analysis were performed as described previously (11).

Luciferase assay. For transcriptional transactivation experiments, MM.1S cells were transfected with 3× HRE, mutated 3× HRE, or empty vector, using amaxa as indicated. At 24 hours after transfection, cells were lysed and luciferase activity was measured using a Dual-Glo Luciferase Assay System (Promega) and Monolight 3010 Luminometer (BD Biosciences), according to the manufacturer's instructions. Reporter activity is presented as percentage of luciferase activity of the 3× HRE reporters relative to the pRL-CMV *Renilla* luciferase control reporter.

ELISA. VEGF levels secreted by MM cells and BMSCs (3×10^5/mL) alone or MM-BMSC cocultures were quantified, as previously described (25). Briefly, for coculture experiments, BMSCs were seeded onto culture plates overnight and MM cell lines were added to BMSC-coated plates the following day. Supernatants were harvested from 24-hour cultures.

Hif-1α functional analysis. Hif-1α transcription factor activity in MM cells was determined with the TransAM Hif-1α kit (Active Motif) according to the manufacturer's instructions (Active Motif). Briefly, Hif-1α dimers in nuclear extracts specifically bind to an oligonucleotide containing the hypoxia-response element immobilized on a 96-well plate and are identified by means of an anti–Hif-1α antibody. Wild-type (wt) consensus oligonucleotide was used as a competitor for Hif-1α binding to monitor the specificity of the assay. The use of a mutated consensus oligonucleotide served as an additional negative control. Nuclear extracts of $CoCl_2$-stimulated COS-7 nuclear extracts were used as a positive control for Hif-1α activation.

DNA fragmentation assay. Cell death detection ELISAplus (Roche Applied Sciences) was used to quantitate DNA fragmentation, as per manufacturer's instructions.

Zebrafish angiogenesis assay. Zebrafish were bred and maintained as described (26). Hemizygous transgenic *tg(Fli1:eGFP)*^{y1} embryos (27) were kept in E3 buffer (5 mmol/L NaCl, 0.17 mmol/L KCl, 0.33 mmol/L $CaCl_2$, 0.33 mmol/L $MgSO_4$) at 28°C until gastrulation was completed. At 15 h post fertilization (hpf), embryos were placed in E3 buffer containing PTU at a final concentration of 0.2 mmol/L to prevent melanization with 0.5% DMSO, 1 or 5 μmol/L adaphostin. At 44 hpf, embryos were washed with fresh E3 buffer and analyzed by confocal microscopy using a Zeiss LSM 510 META confocal microscope with a 20× Achroplan objective. The experiment was repeated five times with indicated numbers of embryos per treatment group.

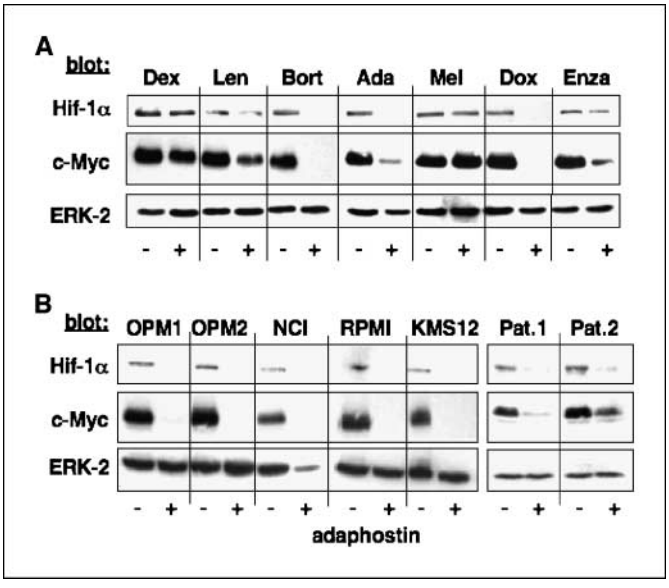

Figure 1. Drug-induced down-regulation of c-Myc and Hif-1α in MM cells. *A,* MM.1S cells were treated (8 h) with dexamethasone (0.5 μmol/L; *Dex*), lenalidomide (0.5 μmol/L; *Len*), bortezomib (1 nmol/L; *Bort*), adaphostin (1 μmol/L; *Ada*), melphalan (0.25 μmol/L; *Mel*), doxorubicin (10 nmol/L; *Dox*), or enzastaurin (2.5 μmol/L; *Enza*), followed by immunoblot analysis of the lysates with indicated antibodies. *B,* adaphostin-induced down-regulation of c-Myc and Hif-1α in MM cell lines and primary cells. MM cell lines were treated with adaphostin (1 μmol/L, 8 h), followed by immunoblot analysis of the lysates with indicated antibodies. Immunoblotting for ERK-2 confirmed equal protein loading.

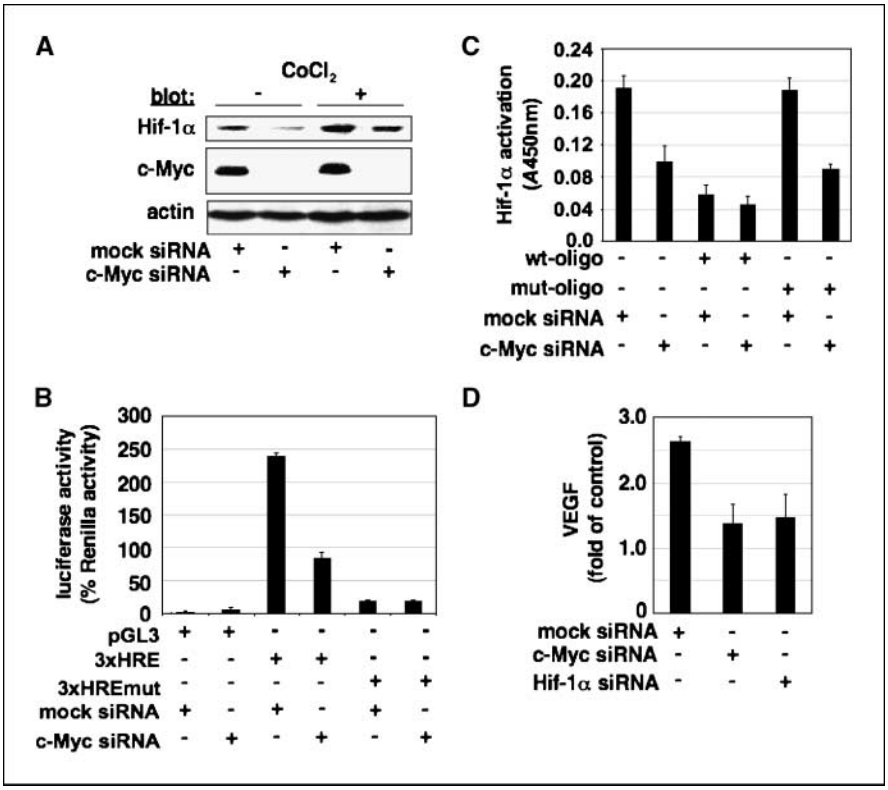

Figure 2. Oncogenic c-Myc collaborates with Hif-1α in MM cells to mediate VEGF secretion. *A,* siRNA-mediated knockdown of c-Myc is associated with Hif-1α down-regulation. MM.1S cells were transiently transfected with either nontargeting control (mock) siRNA (200 nmol/L) or c-Myc siRNA (200 nmol/L) and exposed to $CoCl_2$ (100 μmol/L), followed by immunoblotting with indicated antibodies. Immunoblotting for actin confirmed equal protein loading. *B,* siRNA-mediated knockdown of c-Myc inhibits Hif-1α promoter activity. MM.1S cells were transiently transfected with either nontargeting control (mock) siRNA or c-Myc siRNA together with either empty vector pGL3, 3× wt (*3×HRE*), or mutated HIF-response elements (*3×HREmut*) and a minimal promoter. Transfection mixes also contained a plasmid encoding *Renilla* luciferase for normalization. Luciferase activity was measured after 18 h. *Columns,* averages from triplicate experiments; *bars,* SE. *C,* transient transfection of c-Myc siRNA specifically decreases Hif-1α binding activity. Specific binding of Hif-1α dimers in nuclear extracts to HRE-containing oligonucleotides immobilized on a 96-well plate was inhibited by transient transfection with c-Myc siRNA. Wt consensus oligonucleotide (*wt-oligo*) served as a competitor for Hif-1α binding to monitor the specificity of the assay. The use of a mutated consensus oligonucleotide (*mut-oligo*) served as an additional negative control. The assay was performed on samples transiently transfected with nontargeting control (mock) siRNA and c-Myc siRNA, respectively. *D,* siRNA-mediated knockdown of c-Myc and Hif-1α down-regulate VEGF secretion. MM.1S cells were transiently transfected with 200 nmol/L of mock siRNA, c-Myc siRNA, or Hif-1α siRNA. Supernatants were collected after 18 h and analyzed for VEGF protein by ELISA. *Columns,* mean absorbance of quadruplicate cultures; *bars,* SD.

***In vitro* angiogenesis assay.** The antiangiogenic potential of adaphostin was studied using an *in vitro* angiogenesis assay kit (CHEMICON), as per manufacturer's instructions. Tube formation was assessed using an inverted light/fluorescence microscope at 4× to 10× magnification. Photographs are representative of each group and three independent experiments.

Xenograft mouse model. Beige-nude Xid mice were inoculated s.c. with 3×10^7 MM.1S MM cells in 100 μL RPMI 1640, together with 100 μL Matrigel (BD Biosciences; ref. 28). When tumor was measurable, mice were assigned to the adaphostin treatment group or a control group. Adaphostin was dissolved in PEG 300 and given twice per week by i.p. injection. The control group received the carrier alone at the same schedule and route of administration. Tumor burden was measured every alternate day using a caliper [calculated volume = $4\pi/3 \times (\text{width} / 2)^2 \times (\text{length} / 2)$]. Animals were sacrificed when their tumor reached 2 cm or when the mice became moribund. Overall survival (OS) in animal studies was measured using the Kaplan-Meier and log-rank method. Results are presented as the median OS, with 95% confidence intervals. All animal studies were approved by the Dana-Farber Animal Care and Use Committee.

Immunohistochemistry. Four-micron-thick sections of formalin-fixed tissue were used for TUNEL staining and staining with CD31 antibody (BD Pharmingen) in a humid chamber at room temperature, as in prior studies (11). For image capturing, the LEICA DMIL microscope was connected to a Leica DFC 300FX digital camera and exported to Leica IM50 Image Manager Software. Leica N Plan 5×/0.12 PH0, Leica N Plan 10×/0.25 PH1, and Leica HCX PL Fluotar 40×/0.60 corr PH2 XT objective lenses were used.

Microarray analysis and statistics. Expression data for plasma cells derived from healthy donors and from 65 MM patients were derived from a study by Carrasco and colleagues (29). For the survival analysis, data were derived from a study by Zhan and colleagues (ref. 30; see Supplementary Fig. S2 for a detailed description of methodologies used).

Results

Drug-induced down-regulation of c-Myc is associated with decreases of constitutively elevated Hif-1α levels in MM. While Hif-1α inhibits physiologic c-Myc activity, it collaborates with oncogenic c-Myc to induce VEGF expression in a variety of cancer cells (18, 19). However, the functional relationship of c-Myc and Hif-1α in MM and BM angiogenesis, as well as its potential as a target for novel and investigative anti-MM agents, is unknown. We therefore first screened conventional and novel anti-MM agents for their ability to decrease c-Myc and Hif-1α levels.

Our results show strong down-regulation of both c-Myc and Hif-1α after a low-dose and short-time treatment with bortezomib, doxorubicin, and adaphostin (20, 21, 31), as well as moderate down-regulation triggered by a low-dose treatment with PKC

inhibitor enzastaurin (32–35) and the immunomodulatory drug lenalidomide (36). In contrast, no changes of c-Myc and Hif-1α protein levels were observed after treatment with dexamethasone or melphalan (Fig. 1*A*). We chose adaphostin as a representative drug, which down-regulates c-Myc and Hif-1α to further delineate potential c-Myc/Hif-1α–associated molecular sequelae. To validate our data obtained in MM.1S cells, we first tested c-Myc and Hif-1α protein levels in other MM cell lines (OPM1, OPM2, NCI-H929, RPMI8226, KMS12) and primary MM cells before and after treatment. High baseline c-Myc and Hif-1α levels were confirmed in all MM cell lines and primary MM cells investigated. Moreover, treatment with adaphostin, at doses as low as 1 μmol/L, significantly reduced both c-Myc and Hif-1α levels (Fig. 1*B*), without affecting overall cell survival at these early time points (Supplementary Fig. S1). Taken together, our data show that low-dose conventional, novel, and investigational agents, including adaphostin, induce decreased c-Myc and Hif-1α in MM cells.

Oncogenic c-Myc collaborates with Hif-1α to trigger VEGF production and secretion. To evaluate the functional interrelation of c-Myc and Hif-1α in MM, we next transfected MM.1S cells with a pool of siRNA directed against c-Myc and tested for Hif-1α expression. As a control, cells were treated with hypoxia-mimicking $CoCl_2$ (100 μmol/L), which increased baseline levels of Hif-1α. In contrast to previous reports, which show Hif-1α–dependent c-Myc regulation (37–39), our results show that siRNA-mediated knockdown of c-Myc is associated with decreased Hif-1α protein levels, both under normoxic and hypoxic conditions (Fig. 2*A*). Despite these decreased protein levels, no change was observed in cell survival or proliferation at this early time point (data not shown). Consequently, siRNA-mediated knockdown of c-Myc induced significant down-regulation of Hif-1α–dependent HRE promoter activity. The empty vector pGL3, as well as a construct carrying mutated 3× HRE, served as a negative control (Fig. 2*B*). Moreover, nuclear Hif-1α/HRE binding and Hif-1α activity was determined upon siRNA-mediated knockdown of c-Myc. Our results show that knockdown of c-Myc decreases Hif-1α binding and activity. Assay specificity was monitored by incubating nuclear extracts with a wt consensus oligonucleotide as a competitor and a mutated consensus oligonucleotide, respectively. Indeed, decreased Hif-1α activation was observed using the wt consensus oligonucleotide, but not the mutated consensus oligonucleotide (Fig. 2*C*). These data indicate that baseline expression of Hif-1α in MM cells is c-Myc dependent but additional mechanisms contribute to hypoxia-dependent Hif-1α up-regulation. As expected, siRNA-mediated knockdown of both c-Myc and Hif-1α significantly decreased production and secretion of vascular endothelial growth factor (VEGF), a common Hif-1α target gene and most potent angiogenic factor (Fig. 2*D*). Taken together, our results indicate a role for c-Myc in maintaining high baseline levels of Hif-1α protein and associated VEGF production and secretion. This is also consistent with our finding (Fig. 1*A*) that dexamethasone and melphalan fail to regulate c-Myc

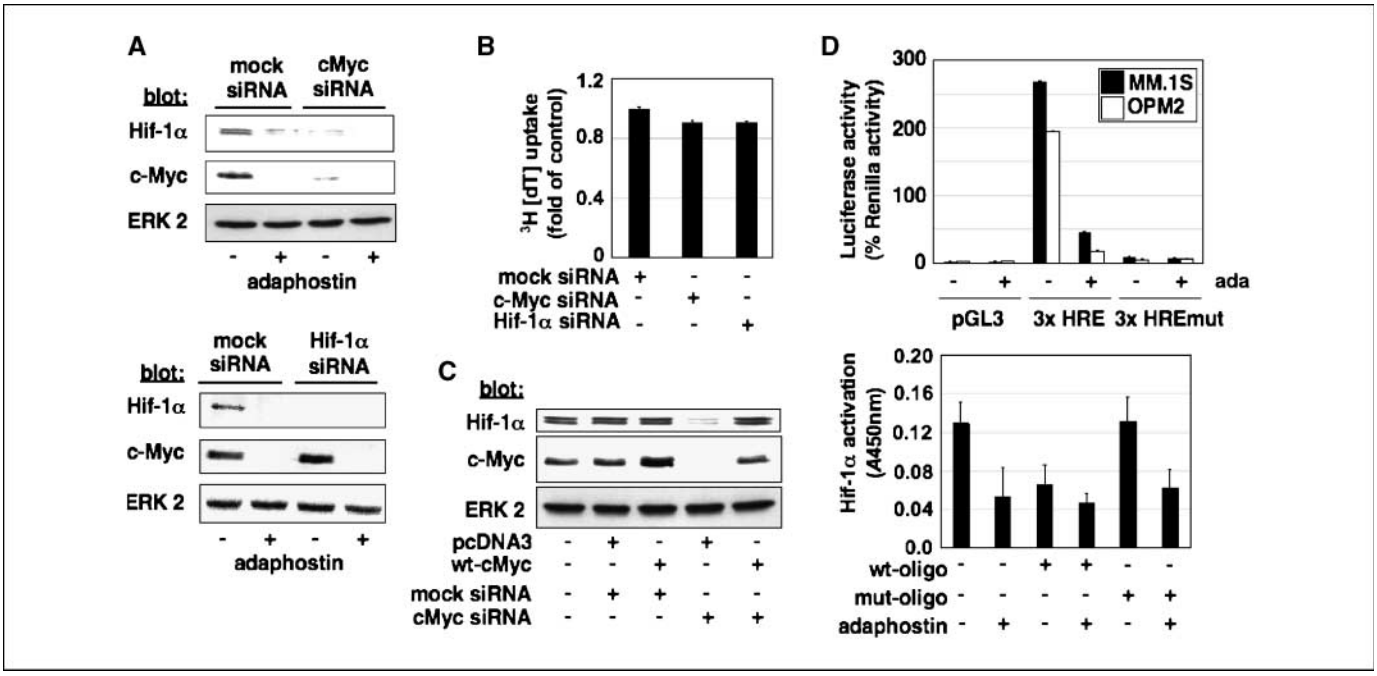

Figure 3. Adaphostin-induced down-regulation of Hif-1α is c-Myc dependent. *A,* Hif-1α is a downstream target of c-Myc. MM.1S cells were transiently transfected with nontargeting control (mock) siRNA or either c-Myc siRNA (200 nmol/L; *top*) or Hif-1α siRNA (200 nmol/L; *bottom*). After 10 h, these cells were treated with adpahostin (1 μmol/L) or left untreated for an additional 8 h and then immunoblotted with Hif-1α and c-Myc. Immunoblotting for ERK-2 confirmed equal protein loading. *B,* transient transfection of c-Myc siRNA or Hif-1α siRNA does not compromise MM cell growth. MM.1S cells were transiently transfected with nontargeting control (mock) siRNA, c-Myc siRNA (200 nmol/L), or Hif-1α siRNA (200 nmol/L), followed by a ^{3}H[dT] uptake assay. *C,* overexpression of wt-c-Myc rescues down-regulation of Hif-1α induced by siRNA-mediated knockdown of c-Myc. At 8 h after transient transfection with c-Myc–specific siRNA (200 nmol/L), MM cells were transfected with a plasmid carrying wt c-Myc. After an additional 10 h, cell lysates were immunoblotted with Hif-1α and c-Myc. Immunoblotting for ERK-2 confirmed equal protein loading. *D,* adaphostin inhibits Hif-1α promoter activity and decreases Hif-1α binding activity. MM.1S and OPM2 cells transiently transfected with either empty vector pGL3, 3× HIF response elements and a minimal promoter (*3×HRE*), or mutated 3× HIF response elements and a minimal promoter (*3×HREmut*) were treated with adaphostin (1 μmol/L, 8 h). Transfection mixes also contained a plasmid encoding *Renilla* luciferase for normalization. Luciferase activity was measured after 18 h. *Columns,* averages from triplicate experiments (*top graph*); *bars,* SE. Specific binding of Hif-1α dimers in nuclear extracts to HRE-containing oligonucleotides immobilized on a 96-well plate was inhibited by adaphostin (1 μmol/L). Wt consensus oligonucleotide (*wt-oligo*) was used as a competitor for Hif-1α binding to monitor the specificity of the assay. The use of a mutated consensus oligonucleotide (*mut-oligo*) served as an additional negative control (*bottom graph*).

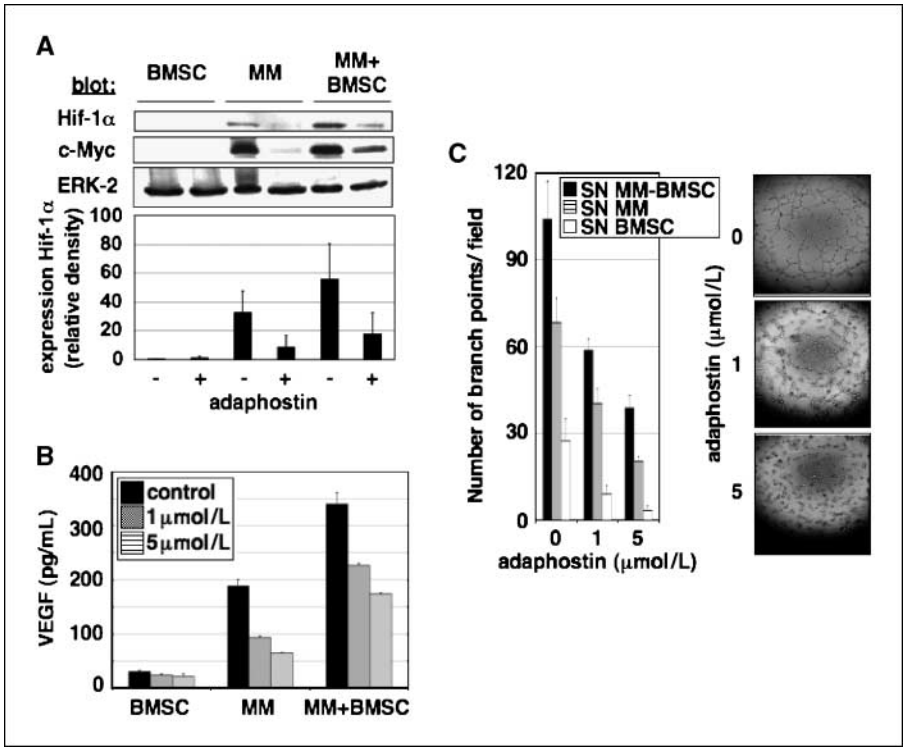

Figure 4. Defining the antiangiogenic activity of adaphostin in the MM microenvironment. *A,* MM cell–BM stromal cell adhesion–induced Hif-1α is inhibited by adaphostin. Lysates of adaphostin-treated and untreated MM.1S cells or MM.1S cells cocultured with BMSCs were analyzed by immunoblotting with antibodies against Hif-1α and c-Myc. Immunoblotting for ERK-2 confirmed equal protein loading. *B,* MM cell–BMSC adhesion–induced VEGF secretion is inhibited by adaphostin. MM.1S cells were cultured in control medium alone or with the indicated concentrations of adaphostin in the presence or absence of BMSCs. Supernatants were collected after 18 h and analyzed for VEGF protein by ELISA. *C,* adaphostin-induced inhibition of endothelial tubule formation. Endothelial cell suspensions were premixed 1:1 with supernatants from experiment in *B* and EGM-2 and added on top of the ECMatrix. Tubule formation was assessed using an inverted light microscope at 4× to 10× magnification. The branching points of endothelial tubule were counted independently by two individuals in several random view fields per well, values were averaged, and statistically significant differences were measured using the Student's *t* test (*left*). Photographs of tubule formation are representative of each group and three independent experiments (*right*).

and Hif-1α protein levels, both of which are weak inhibitors of angiogenesis.

Adaphostin-induced down-regulation of Hif-1α is c-Myc dependent. Our data show that c-Myc regulates Hif-1α protein levels. Specifically, transient knockdown of c-Myc down-regulates Hif-1α protein levels (Fig. 3*A, top graph*). In contrast, transient knockdown of Hif-1α does not affect c-Myc protein levels (Fig. 3*A, bottom graph*). Importantly, the rate of proliferation under these conditions was not compromised (Fig. 3*B*). Transfection of a plasmid carrying wt c-Myc 8 hours after siRNA-mediated knockdown of c-Myc rescued decreases in Hif-1α levels, further showing that Hif-1α is downstream of c-Myc (Fig. 3*C*). Similar to Hif-1α down-regulation triggered by c-Myc knockdown, treatment of MM.1S and OPM.2 MM cells with low-dose adaphostin (1 μmol/L) inhibits Hif-1α–dependent HRE– promoter activity. The empty vector pGL3, as well as a construct carrying mutated 3× HRE, served as a negative control (Fig. 3*D, top graph*). Moreover, our results show that, similar to knockdown of c-Myc, adaphostin specifically decreases Hif-1α binding and activity (Fig. 3*D, bottom graph*). Taken together, these data are consistent with a model of c-Myc–dependent decreases of Hif-1α protein levels and support the potential to therapeutically target this relationship.

Defining the antiangiogenic activity of adaphostin in MM. We next sought to translate these effects in a preclinical *in vitro* MM model. Given that VEGF production and secretion is increased in cocultures of MM cells with BMSCs (40), we investigated whether adhesion of MM cells to stromal cells modulates c-Myc and Hif-1α protein levels. Our results show that Hif-1α levels are significantly elevated upon binding of MM cells to BMSCs (Fig. 4*A*). Similar to hypoxia, additional c-Myc–independent mechanisms contribute to the regulation of Hif-1α levels in MM cells, as evidenced by increased Hif-1α but not c-Myc expression when cocultured with BMSCs. By decreasing c-Myc and Hif-1α levels in the cocultures, adaphostin inhibits VEGF production and secretion triggered by MM cell binding to BMSCs (Fig. 4*B*). Consistent with these results, tubule formation stimulated with supernatants derived from the experiment in Fig. 4*B* (5 hours) was markedly inhibited by adaphostin (Fig. 4*C*).

In summary, inhibition of c-Myc–dependent Hif-1α levels by adaphostin in the BM microenvironment is followed by decreased production and secretion of VEGF, the key growth factor for endothelial cells.

Validating the antiangiogenic activity of adaphostin in a zebrafish model. To further confirm the antiangiogenic activity of our tool compound, adaphostin, *in vivo*, we additionally used an established zebrafish model (*Danio rerio*). When compared with the rabbit cornea and chick embryo chorioallantoic membrane assays, the zebrafish model shows equal capacities to discriminate antiangiogenic compounds more rapidly at 24 to 48 h with higher screening capacity. The most important advantage of performing studies of angiogenesis in the zebrafish is its high transparency and the availability of *tg(Fli1:eGFP)*^{y1} embryos with enhanced green fluorescent protein expression in endothelial cells lining the blood vessels (27, 41, 42). The zebrafish angiogenesis assay is based on the real-time evaluation of blood vessel formation in a live zebrafish embryo. At 24 hpf, the major vessels (dorsal aorta, posterior cardinal vein) are formed by vasculogenesis. Subsequently, the intersegmental vessels (ISV), parachordal vessels (PAV), and the dorsal longitudinal anastomotic vessels (DLAV) develop along the trunk by sprouting angiogenesis. Hemizygous *tg(Fli1:eGFP)*^{y1} embryos (27, 41, 42) at 15 hpf were treated for 30 hours with adaphostin at doses as low as 1 and 5 μmol/L or DMSO. Our results show significant concentration-dependent inhibition of vessel formation, particularly the PAVs, DLAVs, and ISVs, predominantly in the anterior trunk of the fish, whereas the formation of the major blood vessels was unaffected. These observations indicate that adaphostin selectively mediates inhibition of angiogenic vessel sprouting, because the formation of other tissues seems intact (Fig. 5; Supplementary

Fig. S2). Importantly, the inhibition of vessel formation is reminiscent of previous reports testing VEGF inhibitors in the zebrafish model (42–44).

Activity of adaphostin using a MM xenograft mouse model. Finally, we sought to translate the antiangiogenic and antiproliferative effects of adaphostin in a preclinical model of MM. Immunedeficient beige-nude-xid mice were inoculated s.c. with 3×10^7 MM.1S cells and randomized into a control and a treatment (10 mg/kg) group. When tumors reached a palpable size, adaphostin was given i.p. weekly over a 6-week period and then maintained until tumor size required sacrifice. Tumor growth was almost completely inhibited (Fig. 6*A*) in adaphostin-treated mice versus control mice. Using Kaplan-Meier and log-rank analysis, the mean OS was 21 days in the control cohort versus 63 days in the treatment group. Statistically significant prolongation in mean OS was observed in treated animals compared with control mice ($P = 0.006$; Fig. 6*B*). Neither treatment with the vehicle alone nor adaphostin affected the animals' body weight (Fig. 6*C*). Consistent with data obtained in the zebrafish, tumor angiogenesis was markedly reduced within tumors of adaphostin-treated versus nontreated mice, as evidenced by CD31 staining of tumors at day 21. Concomitantly, c-Myc, Hif-1α, and VEGF expression were decreased (Fig. 6*D, IHC*). After treatment discontinuation, there was a rapid increase of tumor angiogenesis, expression of c-Myc, Hif-1α, and VEGF (Fig. 6*D, IHC* and *right top graph*), as well as tumor growth (Fig. 6*D, right bottom graph*) determined at day 32 after stopping treatment. These data support a key role of tumor angiogenesis in MM and further show that inhibition of angiogenesis contributes to the previously reported anti-MM activity of adaphostin (22).

Interestingly, the HIF1A gene encoding Hif-1α showed a significant increased expression ($P = 0.02$, Mann-Whitney test) in tumor cells versus plasma cells derived from healthy donors (29). In several samples, HIF1A showed a lower expression than the healthy controls, whereas a subset showed high levels of expression. When the association of HIF1A overexpression with prognosis was tested on a published data set of 559 MM patients (30), a significant link between HIF1A overexpression and poor prognosis was found ($P = 0.0069$; Supplementary Figs. S3 and S4). These data further point to the possible relevance of HIF1A and, eventually, the activation of general hypoxic mechanisms in the progression of a subset of MM

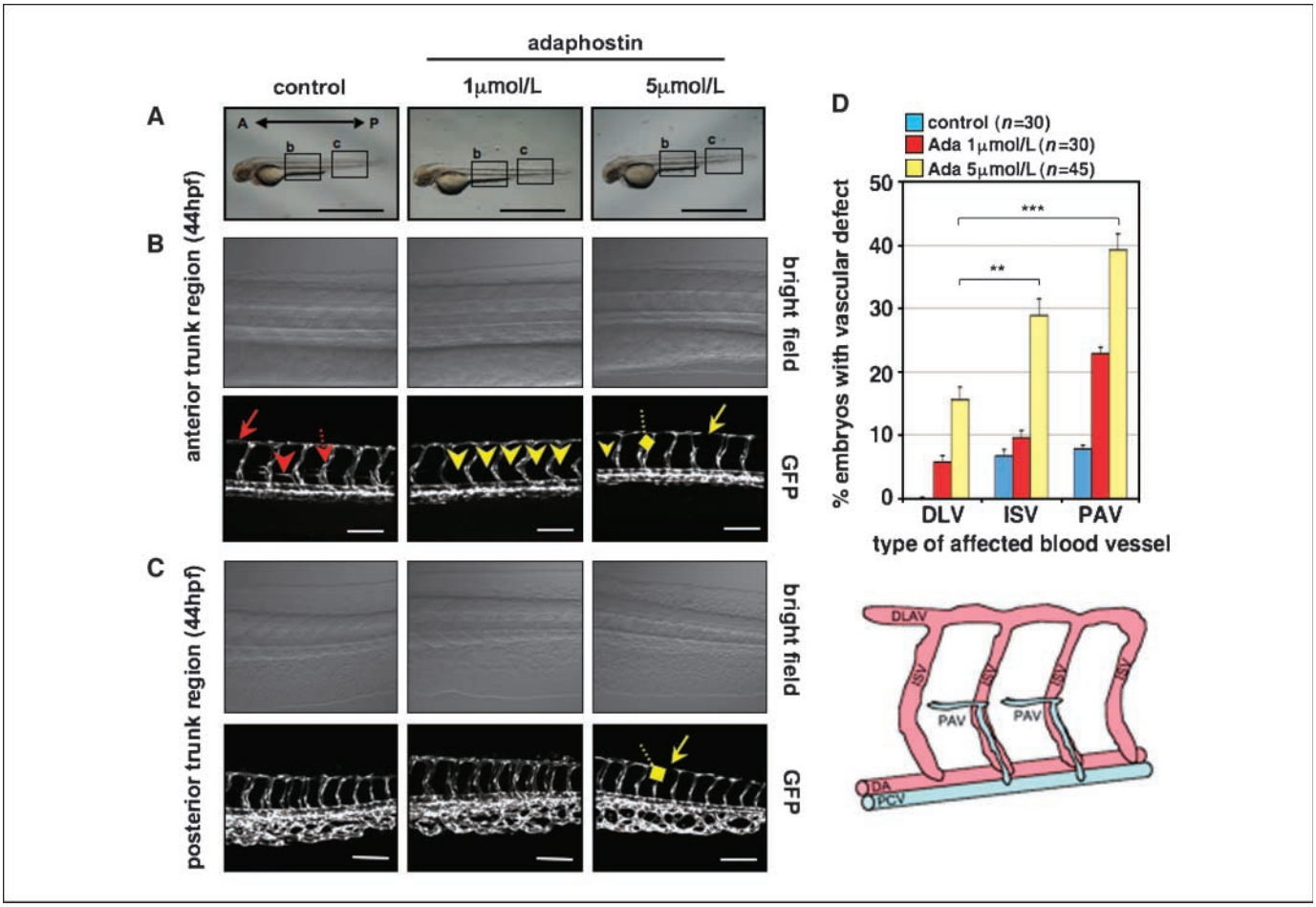

Figure 5. Validating the antiangiogenic activity of adaphostin in a zebrafish model. *A,* bright field images of adaphostin-treated full-length *TG(fli1:EGFP)*^{y1} embryos at 44 hpf. Lateral views, dorsal up: *left,* anterior (*A*); *right,* posterior (*P*). Boxed areas labeled *b* and *c* indicate anterior and posterior trunk regions shown in *B* and *C*, respectively. *Scale bar,* 1 mm. *B* and *C,* confocal projections showing lateral views of somites of anterior (*B*) and posterior (*C*) trunk. *Top,* transmitted light images; *bottom,* fluorescent images. *Arrows,* DLAV; *arrowheads,* PAV; *diamond arrows,* ISV; *red arrows,* intact vessels; *yellow arrows,* defect/missing vessels. *Scale bar,* 1 mm. Representative images of one embryo in each treatment group and five independent experiments are shown. *D,* vascular defects within the zebrafish trunk region, including PAVs, DLAVs, and ISVs, were scored independently by two individuals in nontreated/control ($n = 30$) and adaphostin-treated (1 μmol/L, $n = 30$; 5 μmol/L, $n = 45$) embryos. **, two-tailored Student's *t* test ($P = 0{,}0011$); ***, two-tailed Student's *t* test ($P = 0{,}0005$). SD was calculated from three technical replica. Scheme of zebrafish vessels.

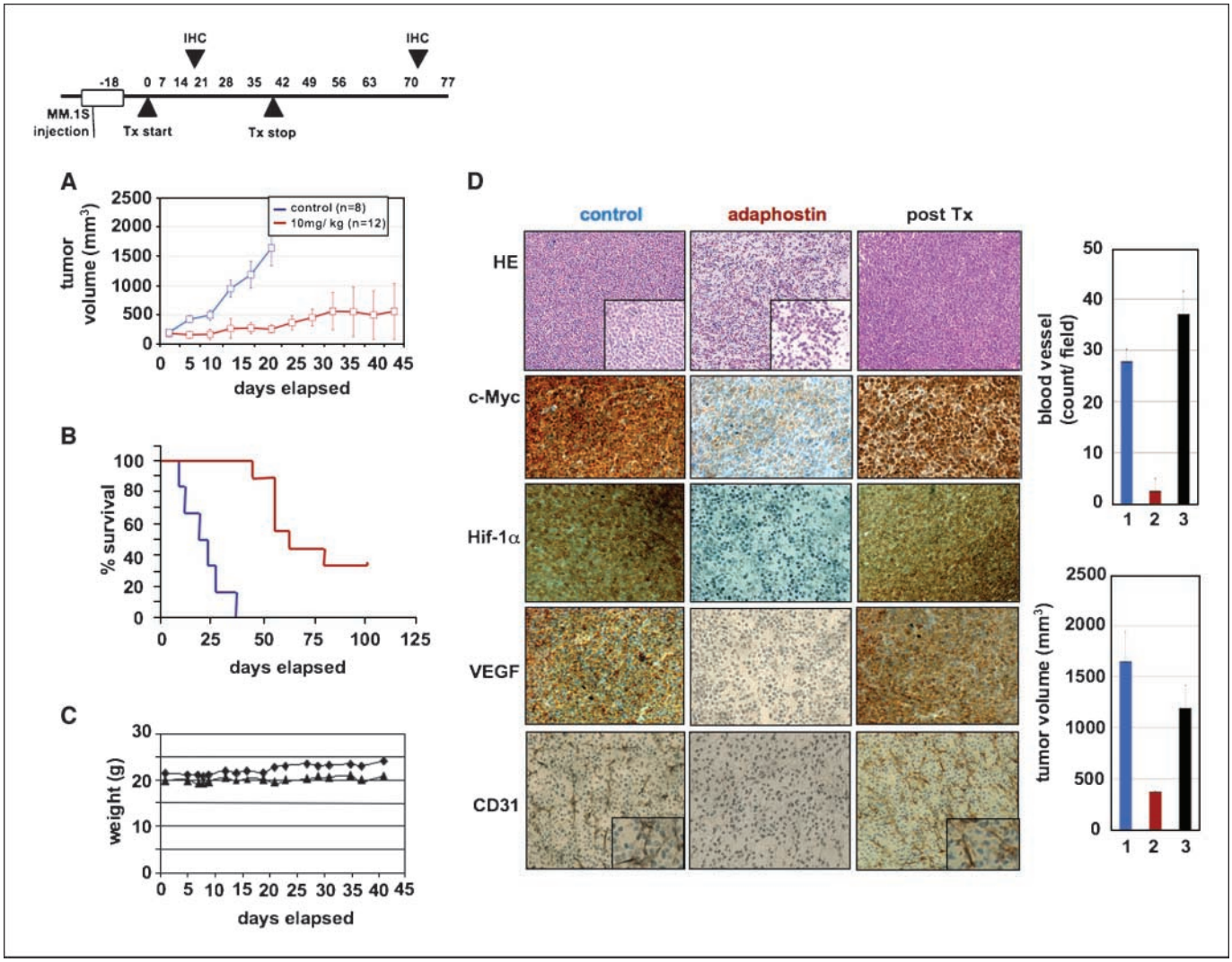

Figure 6. Adaphostin induces down-regulation of c-Myc and Hif-1α in a MM xenograft mouse model and is associated with decreases of VEGF, tumor angiogenesis, and tumor growth and survival. Beige-nude Xid mice were inoculated s.c. in the right flank with 3×10^7 MM.1S cells. Treatment i.p. (vehicle alone or 10 mg/kg adaphostin once weekly) was started when tumors were measurable. *A,* tumor burden was measured every alternate day using a caliper. *Points,* mean tumor volume; *bars,* SE. *B,* survival was evaluated using Kaplan-Meier curves and log-rank analysis. *C,* body weight was evaluated thrice a week. *D,* representative microscopic images of tumor sections are shown stained with H&E [magnification, 4× and 10× (insert)], c-Myc, Hif-1α, VEGF, and CD31 [magnification, 10× and 40× (inserts)]. Blood vessels were quantified in tumor sections from control mice (*1*), mice treated with adaphostin (*2*), or mice after discontinuation of treatment (*3*). Blood vessels were enumerated independently by two individuals in nonnecrotic areas of each section using light microscopy (*right top graph*). Tumor volume was measured in nontreated control mice (at treatment day 21; *1*), adaphostin-treated mice (at treatment day 21; *2*), and adaphostin-treated mice at day 32 after discontinuation of treatment (*3*; *right bottom graph*).

patients. Because HIF1A does not reside within regions of amplification and has not been previously implicated in chromosomal translocations in MM, other mechanisms of overexpression might be active in MM cells.

Taken together, these results strongly support a pivotal role for Hif-1α in MM pathogenesis. Moreover, these mechanisms may also play a role in other malignancies. Indeed, similar to MM, Hif-1α levels are increased in a variety of other tumors, including colon, breast, gastric, lung, skin, ovarian, pancreatic, prostate, and renal carcinomas, and are associated with increased patient mortality (14).

Discussion

Complex karyotypic abnormalities of the c-myc locus have been reported in MM cell lines and in nearly 40% of MM cells from patients with advanced disease (7). A key role for c-Myc in MM pathogenesis has been proposed (8, 9). However, functional mechanisms of c-Myc mediating disease progression are not fully elucidated, and a role of c-Myc in triggering MM BM angiogenesis may be one contributing factor (5, 6, 10).

Here, we show a link between oncogenic c-Myc and Hif-1α expression, VEGF production, and poor prognosis in MM patients. Specifically, c-Myc and Hif-1α are elevated in all MM cells, even under normoxic conditions. We have, therefore, screened for a compound that targets Hif-1α and shown that adaphostin, bortezomib, lenalidomide, and enzastaurin decrease Hif-1α levels and VEGF, dependent on c-Myc. Drug-induced decreases in c-Myc and/or Hif-1α levels have also been previously observed in response to 2ME2, 17-AAG, and pazopanib, which are antiangiogenic and effective in MM and/or other solid and hematologic malignancies (11, 33, 45–49).

Functionally, the particular novelty of our data is the demonstration that Hif-1α protein level and activity in MM cells under normoxic conditions is regulated by oncogenic c-Myc to influence VEGF secretion and angiogenic activity. Our findings are consistent with previous studies in other tumor models showing that oncogenic c-Myc collaborates with Hif-1α to induce the expression of VEGF (angiogenesis; refs. 5, 6, 10, 18, 19) but in contrast to previous reports that show Hif-1α–dependent c-Myc regulation (37–39). In ongoing studies, we are investigating both c-Myc–dependent molecular mechanisms, which regulate the maintenance of Hif-1α levels in the MM cell, including transcriptional, translational, and posttranslational modifications, as well as initial events leading to drug (e.g., adaphostin)–induced decreases of c-Myc and Hif-1α. Of note, although adaphostin induces ROS release in MM cells, pretreatment with PDTC did not abrogate adaphostin-induced down-regulation of c-Myc and Hif-1α. These results, therefore, exclude the possibility that adaphostin-induced effects on c-Myc and Hif-1α are due to protein degradation (data not shown).

After defining a role of c-Myc and Hif-1α in *in vitro* MM BM models, we subsequently validated the *in vivo* antiangiogenic activity of our tool compound, adaphostin (20), using the zebrafish model. Indeed, adaphostin inhibits these sequelae, showing specificity in blocking angiogenesis in zebrafish embryos when used in low doses. To further enhance the clinical relevance of this model, we are now establishing a xenograft zebrafish model for MM, similar to those previously described for other cancers (50). Importantly, adaphostin showed efficacy in a clinically relevant *in vivo* murine xenograft model of human MM, which has predicted the utility of other novel therapies in MM.

Taken together, our studies delineate a new c-Myc/Hif-1α–dependent pathway, which triggers the release of VEGF and the induction of MM angiogenesis and support the hypothesis that oncogenic c-Myc triggers MM progression, at least in part, by modulation of tumor angiogenesis. We, therefore, identify a pivotal role for c-Myc and Hif-1α in MM pathogenesis and provide the framework for clinical trials of new agents, which decrease c-Myc and Hif-1α in MM cells and their BM microenvironment.

Disclosure of Potential Conflicts of Interest

K.C. Anderson: consultant and research support, Celgene and Novartis. The other authors declared no potential conflicts of interest.

Acknowledgments

Received 12/4/08; revised 3/16/09; accepted 4/6/09; published OnlineFirst 6/9/09.

Grant support: Multiple Myeloma Research Foundation Senior Research Grant Award and Dunkin' Donuts Rising Star Award (K. Podar); NIH grants IP50 CA 100707, RO-1 CA 50947, and PO-1 78378 and LeBow Family Fund to Cure Myeloma (K.C. Anderson); and NIH grant CA134660-01 (M. Sattler).

The costs of publication of this article were defrayed in part by the payment of page charges. This article must therefore be hereby marked *advertisement* in accordance with 18 U.S.C. Section 1734 solely to indicate this fact.

We thank Drs. S. Nicoli, S. Schlisio, and M.S. Rodrigues for helpful discussions; M. Zheng for expert help with IHC; and all the members of LeBow Institute for Myeloma Therapeutics and Jerome Lipper Multiple Myeloma Research Center for helpful discussions.

J.Z. designed and performed the experiments; M.S. and G.T. analyzed data and wrote the paper; C.G. performed experiments and wrote the paper; S.L. analyzed data; A.Z., M.S.R., and S.V. performed experiments; Y.Z. and M-A.C. contributed vital data; T.H., Y.T.T., and D.C. analyzed data; K.C.A. analyzed data and wrote the paper; K.P. designed and performed experiments, analyzed data, and wrote the paper.

References

1. Podar K, Anderson KC. The pathophysiologic role of VEGF in hematologic malignancies: therapeutic implications. Blood 2005;105:1383–95.
2. Pelengaris S, Khan M, Evan GI. Suppression of Myc-induced apoptosis in β cells exposes multiple oncogenic properties of Myc and triggers carcinogenic progression. Cell 2002;109:321–34.
3. Src homology and collagen (protein) (Shc)hors K, Evan G. Tumor angiogenesis: cause or consequence of cancer? Cancer Res 2007;67:7059–61.
4. Pelengaris S, Khan M, Evan G. c-MYC: more than just a matter of life and death. Nat Rev 2002;2:764–76.
5. Baudino TA, McKay C, Pendeville-Samain H, et al. c-Myc is essential for vasculogenesis and angiogenesis during development and tumor progression. Genes Dev 2002;16:2530–43.
6. Knies-Bamforth UE, Fox SB, Poulsom R, Evan GI, Harris AL. c-Myc interacts with hypoxia to induce angiogenesis *in vivo* by a vascular endothelial growth factor-dependent mechanism. Cancer Res 2004;64:6563–70.
7. Shou Y, Martelli ML, Gabrea A, et al. Diverse karyotypic abnormalities of the c-myc locus associated with c-myc dysregulation and tumor progression in multiple myeloma. Proc Natl Acad Sci U S A 2000;97:228–33.
8. Cheung WC, Kim JS, Linden M, et al. Novel targeted deregulation of c-Myc cooperates with Bcl-X(L) to cause plasma cell neoplasms in mice. J Clin Invest 2004;113:1763–73.
9. Chesi M, Robbiani DF, Sebag M, et al. AID-dependent activation of a MYC transgene induces multiple myeloma in a conditional mouse model of post-germinal center malignancies. Cancer Cell 2008;13:167–80.
10. Mezquita P, Parghi SS, Brandvold KA, Ruddell A. Myc regulates VEGF production in B cells by stimulating initiation of VEGF mRNA translation. Oncogene 2005;24:889–901.
11. Podar K, Tonon G, Sattler M, et al. The small-molecule VEGF receptor inhibitor pazopanib (GW786034B) targets both tumor and endothelial cells in multiple myeloma. Proc Natl Acad Sci U S A 2006;103:19478–83.
12. Semenza GL. Targeting HIF-1 for cancer therapy. Nat Rev 2003;3:721–32.
13. Maxwell PH, Wiesener MS, Chang GW, et al. The tumour suppressor protein VHL targets hypoxia-inducible factors for oxygen-dependent proteolysis. Nature 1999;399:271–5.
14. Zhong H, De Marzo AM, Laughner E, et al. Overexpression of hypoxia-inducible factor 1α in common human cancers and their metastases. Cancer Res 1999;59:5830–5.
15. Shin DH, Chun YS, Lee DS, Huang LE, Park JW. Bortezomib inhibits tumor adaptation to hypoxia by stimulating the FIH-mediated repression of hypoxia-inducible factor-1. Blood 2008;111:3131–6.
16. Colla S, Tagliaferri S, Morandi F, et al. The new tumor-suppressor gene inhibitor of growth family member 4 (ING4) regulates the production of proangiogenic molecules by myeloma cells and suppresses hypoxia-inducible factor-1 α (HIF-1α) activity: involvement in myeloma-induced angiogenesis. Blood 2007;110:4464–75.
17. Asosingh K, De Raeve H, de Ridder M, et al. Role of the hypoxic bone marrow microenvironment in 5T2MM murine myeloma tumor progression. Haematologica 2005;90:810–7.
18. Gordan JD, Thompson CB, Simon MC. HIF and c-Myc: sibling rivals for control of cancer cell metabolism and proliferation. Cancer Cell 2007;12:108–13.
19. Dang CV, Kim JW, Gao P, Yustein J. The interplay between MYC and HIF in cancer. Nat Rev 2008;8:51–6.
20. Avramis IA, Christodoulopoulos G, Suzuki A, et al. *In vitro* and *in vivo* evaluations of the tyrosine kinase inhibitor NSC 680410 against human leukemia and glioblastoma cell lines. Cancer Chem Pharmacol 2002;50:479–89.
21. Chandra J, Tracy J, Loegering D, et al. Adaphostin-induced oxidative stress overcomes BCR/ABL mutation-dependent and -independent imatinib resistance. Blood 2006;107:2501–6.
22. Podar K, Raab MS, Tonon G, et al. Up-regulation of c-Jun inhibits proliferation and induces apoptosis via caspase-triggered c-Abl cleavage in human multiple myeloma. Cancer Res 2007;67:1680–8.
23. Yan Q, Bartz S, Mao M, Li L, Kaelin WG, Jr. The hypoxia-inducible factor 2α N-terminal and C-terminal transactivation domains cooperate to promote renal tumorigenesis *in vivo*. Mol Cell Biol 2007;27:2092–102.
24. Ricci MS, Jin Z, Dews M, et al. Direct repression of FLIP expression by c-myc is a major determinant of TRAIL sensitivity. Mol Cell Biol 2004;24:8541–55.
25. Podar K, Tai YT, Davies FE, et al. Vascular endothelial growth factor triggers signaling cascades mediating multiple myeloma cell growth and migration. Blood 2001;98:428–35.
26. Rhodes J, Hagen A, Hsu K, et al. Interplay of pu.1 and gata1 determines myelo-erythroid progenitor cell fate in zebrafish. Dev Cell 2005;8:97–108.
27. Lawson ND, Weinstein BM. *In vivo* imaging of embryonic vascular development using transgenic zebrafish. Dev Biol 2002;248:307–18.
28. Lentzsch S, Rogers MS, LeBlanc R, et al. *S*-3-aminophthalimido-glutarimide inhibits angiogenesis and growth of B-cell neoplasias in mice. Cancer Res 2002;62:2300–5.
29. Carrasco DR, Tonon G, Huang Y, et al. High-resolution

genomic profiles define distinct clinico-pathogenetic subgroups of multiple myeloma patients. Cancer Cell 2006;9:313–25.

30. Zhan F, Huang Y, Colla S, et al. The molecular classification of multiple myeloma. Blood 2006;108:2020–8.

31. Richardson PG, Anderson KC. Bortezomib: a novel therapy approved for multiple myeloma. Clin Adv Hematol Oncol 2003;1:596–600.

32. Graff JR, McNulty AM, Hanna KR, et al. The protein kinase Cβ-selective inhibitor, Enzastaurin (LY317615. HCl), suppresses signaling through the AKT pathway, induces apoptosis, and suppresses growth of human colon cancer and glioblastoma xenografts. Cancer Res 2005;65:7462–9.

33. Podar K, Raab MS, Zhang J, et al. Targeting PKC in multiple myeloma: *in vitro* and *in vivo* effects of the novel, orally available small-molecule inhibitor enzastaurin (LY317615.HCl). Blood 2007;109:1669–77.

34. Lee KW, Kim SG, Kim HP, et al. Enzastaurin, a protein kinase C β inhibitor, suppresses signaling through the ribosomal S6 kinase and bad pathways and induces apoptosis in human gastric cancer cells. Cancer Res 2008;68:1916–26.

35. Oh Y, Herbst RS, Burris H. Enzastaurin, an oral serine/threonine kinase inhibitor, as second- or third-line therapy of non-small-cell lung cancer. J Clin Oncol 2008; 26:1135–41.

36. Thomas SK, Richards TA, Weber DM. Lenalidomide in multiple myeloma. Best Pract Res 2007;20: 717–35.

37. An WG, Kanekal M, Simon MC, et al. Stabilization of wild-type p53 by hypoxia-inducible factor 1α. Nature 1998;392:405–8.

38. Santore MT, McClintock DS, Lee VY, Budinger GR, Chandel NS. Anoxia-induced apoptosis occurs through a mitochondria-dependent pathway in lung epithelial cells. Am J Physiol 2002;282:L727–34.

39. Jiang BH, Agani F, Passaniti A, Semenza GL. V-SRC induces expression of hypoxia-inducible factor 1 (HIF-1) and transcription of genes encoding vascular endothelial growth factor and enolase 1: involvement of HIF-1 in tumor progression. Cancer Res 1997;57:5328–35.

40. Podar K, Anderson KC. Inhibition of VEGF signaling pathways in multiple myeloma and other malignancies. Cell Cycle (Georgetown, Tex) 2007;6:538–42.

41. Weinstein B. Vascular cell biology *in vivo*: a new piscine paradigm? Trends Cell Biol 2002;12:439–45.

42. Tran TC, Sneed B, Haider J, et al. Automated, quantitative screening assay for antiangiogenic compounds using transgenic zebrafish. Cancer Res 2007; 67:11386–92.

43. Chan J, Bayliss PE, Wood JM, Roberts TM. Dissection of angiogenic signaling in zebrafish using a chemical genetic approach. Cancer Cell 2002;1:257–67.

44. Cross LM, Cook MA, Lin S, Chen JN, Rubinstein AL. Rapid analysis of angiogenesis drugs in a live fluorescent zebrafish assay. Arteriosclero Thromb Vascul Biol 2003;23:911–2.

45. Chauhan D, Li G, Auclair D, et al. Identification of genes regulated by 2-methoxyestradiol (2ME2) in multiple myeloma cells using oligonucleotide arrays. Blood 2003;101:3606–14.

46. Chow JM, Liu CR, Lin CP, et al. Downregulation of c-Myc determines sensitivity to 2-methoxyestradiol-induced apoptosis in human acute myeloid leukemia. Exp Hematol 2008;36:140–8.

47. George P, Bali P, Cohen P, et al. Cotreatment with 17-allylamino-demethoxygeldanamycin and FLT-3 kinase inhibitor PKC412 is highly effective against human acute myelogenous leukemia cells with mutant FLT-3. Cancer Res 2004;64:3645–52.

48. Sunwoo JB, Chen Z, Dong G, et al. Novel proteasome inhibitor PS-341 inhibits activation of nuclear factor-κ B, cell survival, tumor growth, and angiogenesis in squamous cell carcinoma. Clin Cancer Res 2001;7:1419–28.

49. Dredge K, Horsfall R, Robinson SP, et al. Orally administered lenalidomide (CC-5013) is anti-angiogenic *in vivo* and inhibits endothelial cell migration and Akt phosphorylation *in vitro*. Microvasc Res 2005;69:56–63.

50. Nicoli S, Presta M. The zebrafish/tumor xenograft angiogenesis assay. Nat Protocol 2007;2:2918–23.